AIAA JOURNAL
Vol. 42, No. 10, October 2004

New Interfacial Fluid Thickness Approach in Aero-Optics with Applications to Compressible Turbulence

Haris J. Catrakis* and Roberto C. Aguirre†
University of California, Irvine, Irvine, California 92697

A general approach in aero-optics is proposed based on the physical thickness of refractive fluid interfaces. In turbulent flows between dissimilar-index-of-refraction or optically different gas streams, particularly at large Reynolds numbers, the interfacial fluid thickness is highly variable. The role of this interfacial fluid thickness in aero-optical interactions is examined by directly relating the optical path length (OPL) to the interfacial fluid thickness (IFT) variations. This is done by expressing the OPL as an integral of the IFT variations along the beam propagation path. The proposed IFT approach is demonstrated on refractive-field measurements in large Reynolds number ($Re \sim 10^6$) high-compressibility ($M_c \sim 1$) shear layers between optically different gases. Highly irregular networks of isolated high-gradient interfaces are observed at various transverse locations in the flow, that is, both in the interior and near the outer boundaries. The observation that the high-gradient interfaces are spatially isolated and the OPL interpretation in terms of the IFT variations are utilized to propose and demonstrate a new modeling approach for compressible flow where the high-gradient interfaces are the dominant elements needed to capture the large-scale optical distortions. The present approach suggests a new point of view for relating aero-optical distortions to the flow structure in terms of the IFT variations.

I. Introduction

WHENEVER a laser beam of aperture A propagates through a variable-index-of-refraction turbulent flow, its wavefront is aberrated. The imposed aberrations affect the beam's ability to be focused in the far field; this, in turn, reduces the performance of systems that make use of the beam for various missions that include free-space communications and directed-energy projection. A similar problem exists for the inverse problem of imaging. The approach to studying the fluid–optic interaction problem is generally divided into two regimes depending on the propagation distance through the turbulent medium: When the propagation distance, Z, is large compared to A, that is, $Z/A \gg 1$, the problem is referred to as atmospheric propagation; when Z/A is of order 1, the problem is referred to as aero-optics.[1–3] These terminologies have been adopted based on the applications as the field developed. In general, the former can be characterized by relatively low spatial and temporal frequencies and due to the transport of passive scalars, in particular temperature fluctuations in the atmosphere, which in turn have concomitant density/index-of-refraction fluctuations. On the other hand, aero-optics is characterized by higher (often much higher) spatial and temporal frequencies in turbulent boundary and shear layers and can be due to the transport of passive scalars as in the case of mixing layers between two disparate index-of-refraction gas streams, or, in fully-subsonic flows, due to fluid dynamic and thermodynamic effects of flow curvature and velocity fluctuations in turbulent gas flows as in the case of mixing of matched total temperature gas streams, which occur in airflows over subsonic aircraft.[4,5] In the case of shear layers were one or both streams are supersonic, to these effects can be added the effects of shocks. In general, the studies found in the literature are divided into low-speed or incompressible studies for the two-index mixing problem and higher Mach number studies for the fluid dynamic/thermodynamic problem; however, it is possible for both mechanisms to operate simultaneously, as is the case for the flow conditions of Dimotakis et al.[6] Although it is theoretically possible to capture both effects using the interfacial fluid thickness approach that will be described here, the ability to separate the contribution due to the two different effects depends on the disparity in the index of refraction between the two gas streams. In the data used in this paper, the difference in index of refraction of the two streams is sufficiently large that the effects are dominated by two-index mixing. Note that large Reynolds number, high Mach number aero-optics problems involving two-index mixing are in and of themselves relevant to optical propagation through engine affluent streams and window cooling for hypersonic interceptors, for example.

To develop techniques for the prediction and control of aero-optical phenomena in turbulent flows, an improved understanding is needed of the large-scale properties and, for some applications, of the small-scale properties of aero-optical distortions, as well as of the turbulent refractive fluid interfaces that generate these distortions.[1] Practically, the large-scale aero-optical behavior is crucial in all applications involving optical beam propagation or imaging through turbulent shear flows, such as the flows generated by airborne vehicles. The small-scale behavior can also be important for those applications that require high-resolution and/or long-range optical imaging or beam propagation. In addition, it is important to know in practice the behavior of aero-optical interactions at large Reynolds numbers. Furthermore, for high-speed flight, it is also crucial to quantify Mach-number effects on the aero-optical behavior.[3]

The large-scale organized flow behavior is known to provide the dominant aero-optical contributions in both incompressible turbulent mixing flows, such as those between optically different gases[6–8] and matched total temperature weakly compressible turbulent flows.[2,5] At higher flow compressibilities, however, the extent to which the large-scale flow behavior is organized is not well understood.[6,9–11] The large-scale properties of aero-optical distortions at high compressibility, and the manner in which they are related to the fluid interfacial behavior, are also not well understood.

In the present work, we propose an approach to examine aero-optical interactions in terms of the variations in the thickness of refractive-fluid interfaces. Refractive interfaces physically exhibit a thickness given by the inverse of the refractive-index gradient

Presented as Paper 2003-0642 at the 41st Aerospace Sciences Meeting, Reno, NV, 6–9 January 2003; received 21 January 2003; revision received 2 April 2004; accepted for publication 2 April 2004.

*Assistant Professor, Aeronautics and Fluid Dynamics Laboratories, Mechanical and Aerospace Engineering, Henry Samueli School of Engineering; catrakis@uci.edu. Member AIAA.

†Graduate Student, Aeronautics and Fluid Dynamics Laboratories, Mechanical and Aerospace Engineering, Henry Samueli School of Engineering. Member AIAA.

magnitude. This interfacial fluid thickness can be highly nonuniform in turbulent flows, particularly at large Reynolds numbers. The interfacial fluid thickness variations play an important role in aero-optics. In Sec. II, we describe the interfacial fluid thickness (IFT) approach and show that the optical path length (OPL) can be expressed directly in terms of the variations in interfacial fluid thickness. In Sec. III we demonstrate this approach on high-compressibility large Reynolds number shear layers of optically different gases. The high-gradient interfaces are identified, and their behavior is compared to the case of low compressibility. A discussion is included on the issue of mixing vs compressibility effects. In Sec. IV, we propose and demonstrate a new modeling approach in which the high-gradient interfaces are used to produce the large-scale aero-optical distortions at high compressibility. In a companion paper, we examine the small-scale behavior of aero-optical distortions at high compressibility and large Reynolds numbers, by means of a new method for characterizing the scale-local structure of optical wavefronts.[12]

II. Proposed IFT Approach in Aero-Optics

Since the pioneering aero-optics studies by Liepmann,[13,14] it has been recognized that one of the central goals in aero-optics research is to relate the optical-wavefront structure to the fluid mechanical behavior. The optical-wavefront distortions are usefully quantified by the OPL, for many aero-optics applications.[1,5,15–17] The most relevant fluid mechanical quantity in aero-optics is the refractive-index field,

$$n(\boldsymbol{x}, t) \equiv c_0/c(\boldsymbol{x}, t) \geq 1 \tag{1}$$

where $c(\boldsymbol{x}, t)$ is the local speed of light, which is always less than or equal to the speed of light c_0 in vacuum. In turbulent flows, the refractive-index field $n(\boldsymbol{x}, t)$ can be highly nonuniform, particularly at large Reynolds numbers. The propagation of optical wavefronts through refractive-index fields is governed by the eikonal equation, which can be expressed in terms of the OPL as

$$|\nabla(\mathrm{OPL})| = n \tag{2}$$

The eikonal equation is useful to describe fluid–optical interactions as long as the wavelength of light is smaller than the smallest fluid mechanical (turbulent) scale (e.g., Liepmann[14]) and as long as the optical beam energies are low enough to not change the local refractive index.

How is the OPL behavior related physically to the structure of the refractive-index field and in particular the refractive-fluid interfaces? In this section, we present a framework that is useful to address this question by emphasizing the role of the physical thickness of the refractive fluid interfaces in determining the variations in the OPL.

As a starting point, we recall the expression used for the definition of the OPL as an integral of the refractive index along each light ray in geometric optics,[1] that is,

$$\mathrm{OPL}(\boldsymbol{x}, t) \equiv \int_{\mathrm{ray}} n(\ell, t)\, \mathrm{d}\ell \tag{3}$$

where ℓ is the physical distance along the beam propagation path for each light ray. The OPL integral in Eq. (3) corresponds to inverting the eikonal equation (2) for the OPL in terms of the refractive-index field. The aero-optical distortions correspond to the optical path difference (OPD) given by $\mathrm{OPD}(\boldsymbol{x}, t) \equiv \mathrm{OPL}(\boldsymbol{x}, t) - \mathrm{OPL}_{\mathrm{ref}}(\boldsymbol{x}, t)$, where

$$\mathrm{OPL}_{\mathrm{ref}}(\boldsymbol{x}, t) \equiv \int_{\mathrm{ray}} n_{\mathrm{ref}}(\boldsymbol{x}, t)\, \mathrm{d}\ell$$

is the reference OPL that would correspond to the undistorted wavefronts, with n_{ref} a reference refractive index, for example, corresponding to freestream conditions. The optical wavefronts can be represented as isosurfaces of the OPL, that is,

$$\mathrm{OPL}(\boldsymbol{x}, t) = \mathrm{const} \tag{4}$$

as indicated schematically in Fig. 1. In Fig. 1, L_δ is the large-scale traverse extent of the flow and measures the extent of the outermost edges of the turbulent refractive-fluid interfaces. As long as the flow speeds are small relative to the speed of light, and the optical-beam propagation distances are small enough for light to propagate through the flow before it has evolved, it is sufficient to think of the OPL integral in Eq. (3) as involving only the instantaneous spatial structure of the refractive-index field, at each instant in time.

As the optical wavefronts propagate through the nonuniform refractive-index field $n(\boldsymbol{x}, t)$, the aero-optical interactions physically occur across the refractive-fluid interfaces. These are the interfaces on which the refractive index n is constant. It is important to understand the role of these interfaces. Although these fluid interfaces correspond to isosurfaces of the refractive-index field, that is,

$$n(\boldsymbol{x}, t) = \mathrm{const} \tag{5}$$

it is crucial to recognize that the refractive-fluid interfaces will have a physical thickness, whereas the refractive-fluid isosurfaces are geometrical objects with zero thickness. It is the physical thickness of the interfaces that is very important in aero-optics. We can introduce

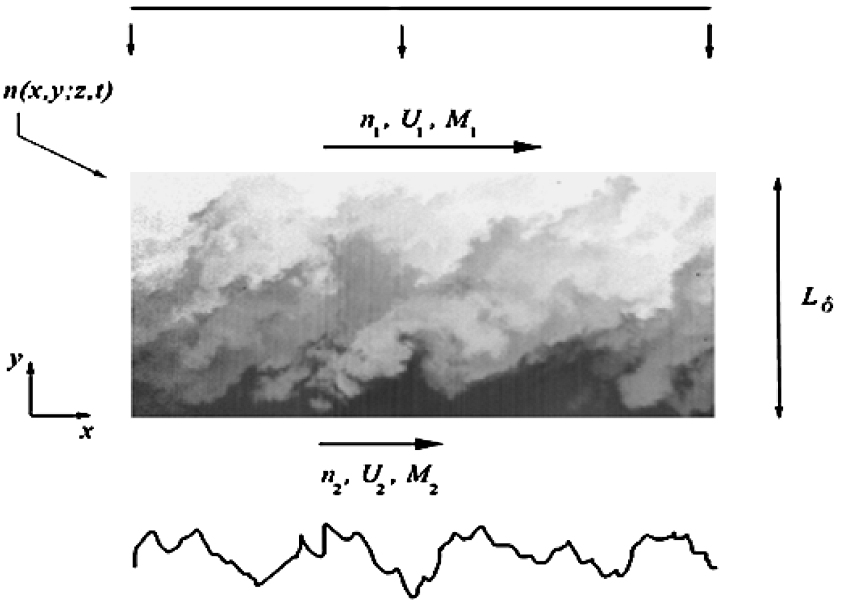

Fig. 1 Schematic of refractive-index field $n(x, y; z, t)$ at high compressibility (gray-level image at the inset), flow from left to right and planar incident optical wavefront (top), propagating from top to bottom, and a propagated distorted optical wavefront (bottom).

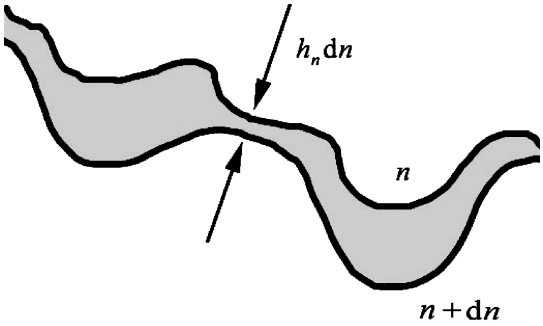

Fig. 2 Schematic of a refractive interface, its interfacial fluid thickness $h_n(x,t)$, and two neighboring isosurfaces of the refractive-index field $n(x,t)$.

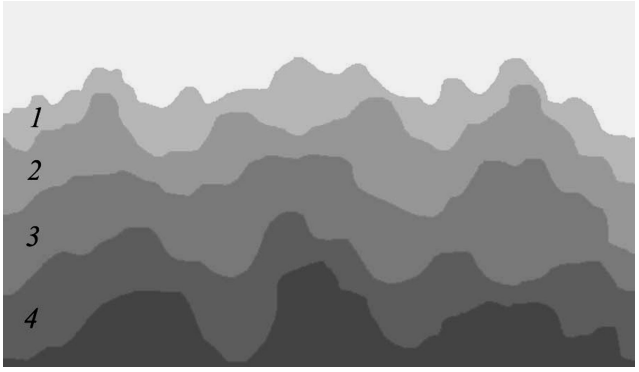

Fig. 3 Schematic of several refractive-fluid interfaces and the variability in the interfacial fluid thickness.

the local IFT h_n, defined per unit n, as the inverse of the refractive-index gradient magnitude, that is,

$$h_n(\boldsymbol{x},t) \equiv 1/|\nabla n| \tag{6}$$

The distance between two neighboring isosurfaces, corresponding to n and $n+\mathrm{d}n$, will be $h_n\,\mathrm{d}n$. This is shown schematically in Fig. 2, for a single interface, and in Fig. 3 for several neighboring interfaces. We can distinguish between the general case, where the gradient magnitude is nonzero, that is, $|\nabla n|>0$, and the special case of zero gradient magnitude, that is, $|\nabla n|=0$, which will be discussed later. In regions of relatively large refractive-index gradients, the isosurfaces are closely spaced and the interfaces are associated with a relatively small thickness. In regions of weak refractive-index gradients, the isosurfaces will be located farther apart and the interfaces will be relatively thicker. The IFT can be expected to be highly nonuniform at large Reynolds numbers. This is because of the strongly intermittent character of fully developed turbulent flows, which becomes more intermittent with increasing Reynolds number for both incompressible and compressible flows.[11,18] As discussed by Jumper and Fitzgerald,[1] refractive-index fluctuations can arise in pure fluids, for example, where density fluctuations are induced by temperature variations in low-speed airflows,[19] or density fluctuations in compressible airflows,[4,5] or in mixtures of dissimilar fluids.[6,20] In all of these different cases, the thickness of the refractive interfaces can be defined in the same manner, that is, using Eq. (6). We note that the present approach could be formulated entirely in terms of the refractive-index gradient. The IFT is especially helpful for physical insight into the aero-optical interactions.

Is the IFT finite? Is it nonzero? In turbulent flows, the IFT can be expected to be both nonzero and finite, in general, on physical grounds. The thickness must be nonzero wherever the local refractive-index gradient magnitude $|\nabla n(\boldsymbol{x},t)|$ is finite, as indicated from Eq. (6). Only an infinite gradient can lead to a zero IFT. Physically, it is clear that for flows of real fluids, even at large but finite Reynolds numbers, the finite molecular diffusivities of the fluid ensure finite gradients and, therefore, finite IFTs. A related observation, also indicated from Eq. (6), is that the thickness must be finite as long as the gradient magnitude is nonzero. If the gradient is zero, which would correspond to a region of exactly uniform refractive index, the thickness would be infinite in the context of Eq. (6) and one then must interpret the (infinity times zero) product $h_n\,\mathrm{d}n$ as a Dirac delta function whose integral becomes the distance given by the extent of the uniform-index region in the direction of the optical ray propagation. In summary, we can expect physically that the IFT must be finite as long as the gradient is finite, consistent with Eq. (6). The thickness is an interfacial property, therefore, that has to be taken into account.

Because each optical ray physically propagates through refractive interfaces, one can intuitively expect that the local IFT should determine, at least in part, the local contribution to the OPL. Can this be seen directly in the OPL integral in Eq. (3)? This can be done by rewriting Eq. (3), from the point of view of the refractive-fluid interfaces, as

$$\mathrm{OPL}(\boldsymbol{x},t) \equiv \int_{\mathrm{ray}} n(\ell,t)h_{n,\ell}|\mathrm{d}n| \tag{7}$$

where the integration is now performed with respect to the refractive index n, rather than with respect to the spatial distance ℓ, and $h_{n,\ell}$ is the effective IFT defined as the component of the interfacial thickness in the direction of optical propagation, given by

$$h_{n,\ell} = 1/|\nabla n|_\ell \tag{8}$$

with $|\nabla n|_\ell$ denoting the effective gradient magnitude, that is, the magnitude of the component of the local refractive-index gradient in the ℓ direction, which is the direction of the optical ray propagation. The component of the refractive-index gradient in Eq. (7) is

$$|\nabla n|_\ell \equiv |\mathrm{d}n|/\mathrm{d}\ell \tag{9}$$

as required for Eqs. (3) and (7) to be consistent. Because the refractive index n could be locally increasing or decreasing as the light rays propagate, it is necessary to express the differential of n as the absolute-valued differential $|\mathrm{d}n|$, in Eq. (7). For interfaces locally normal to the optical rays, the gradient component $|\nabla n|_\ell$ has magnitude identical to the magnitude of $|\nabla n|$. Where the interfaces are locally not perpendicular to the optical rays, this component will be of smaller magnitude than $|\nabla n|$ and the effective IFT will be larger. In other words, the effective gradient is always less than or equal to the full gradient, that is,

$$|\nabla n|_\ell \equiv |\nabla n||\cos\theta| \le |\nabla n| \tag{10}$$

and the effective IFT is always greater than or equal to the full IFT, that is,

$$h_{n,\ell} = 1/|\nabla n|_\ell \equiv h_n|\sec\theta| \ge h_n \tag{11}$$

where the angle θ, taken as $-\pi<\theta\le\pi$, quantifies the interfacial orientation relative to the optical propagation direction.

These considerations provide the basis for the development of a new modeling approach based on the IFT described later in Sec. IV. As long as the refractive-index gradient magnitude is not zero, that is, as long as $|\nabla n|>0$, we can define θ as the angle between the refractive-index gradient vector and the local optical ray propagation vector. The refractive-index gradient vector is always normal to the local refractive interface. Combining Eqs. (11) and (7), we see that the OPL integral of Eq. (3) can be expressed directly in terms of the IFT variations along the optical beam propagation path as

$$\mathrm{OPL}(\boldsymbol{x},t) \equiv \int_{\mathrm{ray}} n(\ell,t)h_n|\sec\theta||\mathrm{d}n| \tag{12}$$

where this integral is in terms of the thickness h_n and relative orientation θ of the refractive interfaces; compare the equivalent integral in Eq. (7). As already mentioned, in the context of the IFT in Eq. (6), these integrals require that $|\nabla n|\neq 0$. In those regions where $|\nabla n|=0$, that is, in regions of uniform refractive index, the

(infinity times zero) product $h_n\,\mathrm{d}n$ must be interpreted again as a Dirac delta function whose integral is the distance, for example, $\Delta\ell$, corresponding to the extent of the uniform-index region in the optical propagation direction, so that the contribution to the OPL integral becomes $\Delta(\mathrm{OPL}) = n\Delta\ell$. We note that, in uniform-index regions, the interfacial orientation θ is not needed. In those instances where the fluid interface happens to be locally tangent to the optical propagation direction, that is, if $\theta = \pm\,\pi/2$, the term $|\sec\theta|$ will be infinite, but in such cases the refractive index will locally be uniform because the interface will be aligned with the optical propagation direction, that is, $|\mathrm{d}n| = 0$ in such cases. In those cases, therefore, the contribution to the OPL integral will again be $\Delta(\mathrm{OPL}) = n\Delta\ell$ with $\Delta\ell$ identified as the length of the interface that is tangential to the optical propagation direction. Also note that, in general, one may also need to take into account other possibilities such as total internal reflection or the development of caustics. These possibilities depend on the magnitudes of refractive gradients, and relative interfacial orientations, encountered in practice.

In summary, the proposed IFT approach is based on relating the OPL to the IFT variations. Whereas the integral in Eq. (3) is conducted over space, the integrals in Eqs. (7) and (12) are expressed as integrals over the refractive index and are helpful to determine the manner in which the refractive interfaces physically contribute to the OPL. In addition to the local refractive index n, the integrals in Eqs. (7) and (12) show that the OPL variations arise from the variability in the interfacial thickness h_n and the fluctuations in the interfacial orientation θ, or the variations in the effective interfacial thickness $h_{n,\ell}$. Knowledge of the variability in the effective interfacial thickness, and its relation to the flow dynamics, can be expected, therefore, to provide physical insight into the relation between the OPL behavior and the interfacial structure.

III. Demonstration on High-Compressibility Turbulent Shear Layer Fluid Interfaces

In this section, we demonstrate the use of the IFT approach on turbulent high-compressibility optically different fluid interfaces. We have chosen to examine the applicability of the proposed approach to high-compressibility fluid interfaces to develop a large-scale aero-optics modeling methodology useful for high-compressibility flow conditions. This will be described in the next section. There are available large-scale aero-optics modeling methods that have successfully addressed weakly compressible flows[1] and incompressible flows.[6,7,21] These methods are based essentially on the Brown-Roshko large-scale organized-structure approach[20] with direct extensions to weakly compressible flows and will be discussed briefly in Sec. IV. It is known, however, that high-compressibility flows are qualitatively different from weakly compressible or incompressible flows.[6,9–11,22,23] A more general approach is desirable, to be able to address aero-optical effects across the full range of compressibilities, and it is toward this goal that the IFT approach of Sec. II can be particularly useful.

Figure 4a shows an example of a two-dimensional spatial streamwise slice of the refractive-index field in a shear layer between optically different gases, with convective Mach number $M_c \sim 1$ and Reynolds number $Re \sim 10^6$ based on the large-scale extent L_δ of the flow.[6] Also shown is an example of a low-compressibility ($M_c \sim 0.2$) shear layer in Fig. 4b, for comparison. These flow images (Fig. 4) span the entire large-scale transverse extent of the flow and, although not fully resolved, they capture a relatively wide range of scales ($\sim$500:1), which permits a study of the large-scale behavior. The imaging technique relies on Rayleigh scattering and on using dissimilar gases that have a large difference in scattering cross section and a relatively large difference in refractive index. The low-speed freestream contains ethylene in both the high- and low-compressibility cases, whereas the high-speed freestream contains helium or nitrogen for the high- or low-compressibility cases, respectively. The freestream refractive-index difference is $\Delta n \sim 6.6 \times 10^{-4}$ or $\Delta n \sim 4.0 \times 10^{-4}$, for the high- or low-compressibility cases, respectively, at the flow conditions investigated. A pulsed laser at a visible wavelength of 532 nm and with energy of $\sim$300 mJ per pulse provided the illumination source for the flow imaging. A description of the flow facility and further details of the experimental technique can be found in Ref. 6.

Note that the refractive-index field in Fig. 4a reflects effects of both mixing and compressibility, as a result of the use of optically different gases, and may not directly represent the density-field behavior, as has been discussed by Jumper and Fitzgerald.[1] The issue of the relative effects of mixing vs density variations is important. It is helpful to appreciate first that nearly uniform concentration regions, in the case of mixing, are consistent with and directly related to low-density wells corresponding to concentrated-vorticity structures, for example, organized vortical structures. Although not directly related, the density-well approach of Fitzgerald and Jumper[5] and the uniformly mixed-region approach of Dimotakis et al.[6] can be viewed in the context of the original Brown–Roshko[20] organized-structures approach because the Brown–Roshko structures, originally recorded at incompressible conditions, are the dominant large-scale vortical structures at low or no compressibility. The density wells associated with these vortical structures become deeper as the level of compressibility rises. Although the underlying fluid mechanics is the same, that is, the same vortical structures generate the low-density wells and the uniformly mixed regions, the magnitude of the aero-optical effects associated with mixing effects vs pure density effects can be expected to be quite different. It is clear that the difference between these two effects, aero-optically, can be large, depending on the choice of the dissimilar gases as opposed to the pure-air total temperature matched freestreams.

The primary emphasis of the present work is on the IFT approach, which is a general approach and can be expected to be useful for studying both mixing and density effects in the future. The data used presently to demonstrate this approach are dominated by the mixing effect but, again, the main approach described in Sec. II is of general use, that is, theoretically, it is not restricted to either effect. The data in Fig. 4a make possible an examination of the IFT approach at high levels of compressibility even though the density-field variations associated with the mixing field can be expected to exhibit features attributable to not only vortical structures, but also compression-wave regions, for example, shocklets, and expansion-wave regions. The refractive-index field in Fig. 4a reflects these flow mechanisms, albeit indirectly, and provides the opportunity to examine the role of high-compressibility fluid interfaces and in particular their physical thickness in generating the aero-optical distortions.

The IFT fields h_n, corresponding to the refractive-index fields n of Figs. 4a and 4b, are shown in Figs. 5a and 5b. The IFT was computed by first evaluating the refractive-index gradient magnitude $|\nabla n|$ and subsequently computing its inverse according to the IFT definition in Eq. (6). The local refractive-gradient magnitudes and IFTs are necessarily under-/overestimated, respectively, because the images are not fully resolved. The computed gradients and thicknesses are essentially coarse-grained values at the image-resolution scale. However, these values permit the relative spatial variations to be examined, and this is what is needed in the present context. Because the refractive-index data of Figs. 5a and 5b are from two-dimensional slices of the flow, only two of the three spatial refractive-index derivatives necessary to evaluate the full gradient magnitude can be computed. The IFT fields in Figs. 5a and 5b, thus, correspond to the in-plane refractive-index gradient magnitude. Note, however, that only the component of the full gradient, or IFT, along the optical ray propagation direction is needed, as is evident in Eqs. (9–11). In other words, even if the full gradient were available, one would compute the component of it in the optical propagation direction, and this would be equivalent to using the in-plane component in addition to the in-plane interfacial orientation, for optical wavefronts propagating in the plane of the flow shown in Figs. 5a and 5b, or Figs. 4a and 4b. In Figs. 5a and 5b, the in-plane gradient magnitudes are shown such that darker regions denote higher values of the gradient magnitude. Because the in-plane interfacial fluid thickness is the inverse of the in-plane gradient magnitude, the darker regions denote locally thin high-gradient interfaces. Also evident in Figs. 5a and 5b are the variations in the interfacial orientation. Depending on the direction of optical beam propagation, the relative interfacial

a)

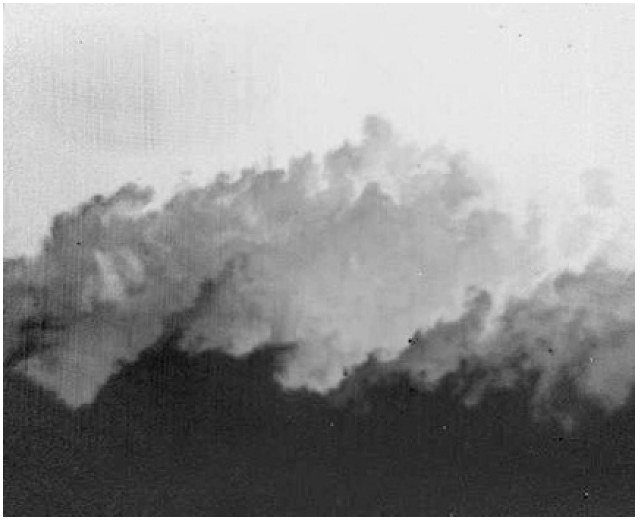

b)

Fig. 4 Refractive-index field a) in a streamwise slice of a high compressibility ($M_c \sim 1$) large Reynolds number ($Re \sim 10^6$) shear layer between optically different gases and b) low compressibility ($M_c \sim 0.2$) shear layer refractive-index field.[6]

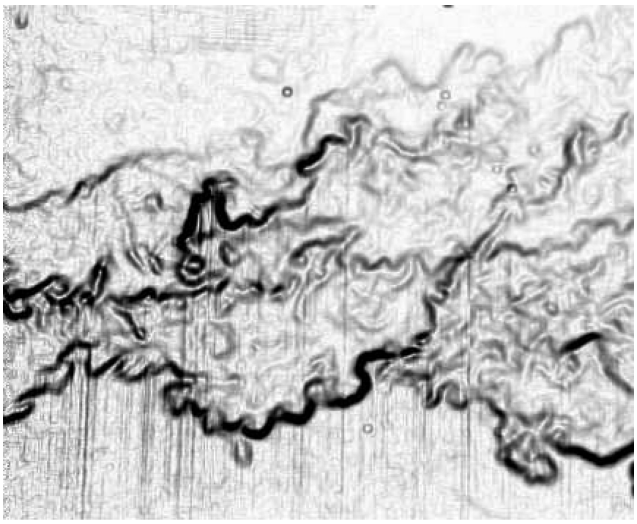

a)

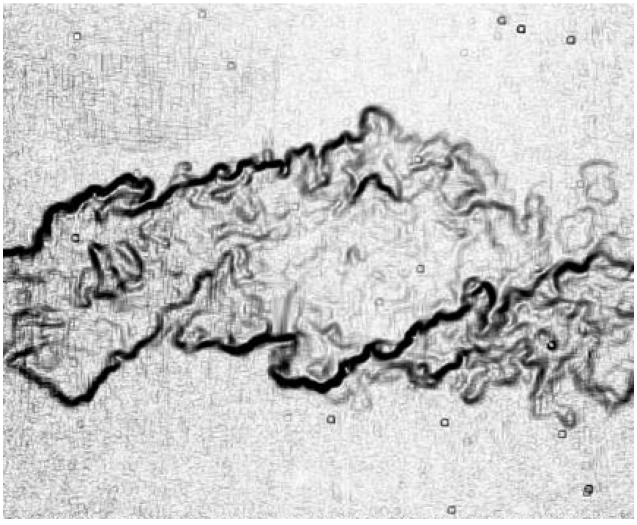

b)

Fig. 5 IFT field h_n at a) high compressibility corresponding to the refractive-index field of Fig. 4a where darker regions denote thinner interfaces, and b) low compressibility corresponding to Fig. 4b.

orientation θ will be different along the beam-propagation path. Figures 5a and 5b indicate, however, that the interfacial orientation is sufficiently irregular that, at least locally, there is a wide distribution of interfacial directions. It is important to recall the meaning of Eqs. (10) and (11), that is, that interfaces of a given thickness will have an effective thickness that is always greater than or equal to it for any optical beam-propagation direction. In other words, a given gradient magnitude will result in an effective gradient magnitude that is always smaller than or equal to it, irrespective of the optical beam-propagation direction. If one identifies, therefore, the regions of high-gradient interfaces in the flow, then there can be no effective gradient magnitudes that are higher yet.

Four significant observations can be made, at high compressibility, on the basis of Fig. 5a and other IFT fields at the same flow conditions:

1) The high-gradient regions occupy a relatively small part of the turbulent shear flow region.

2) The high-gradient regions are sheetlike and can be thought of as high-gradient interfaces.

3) The high-gradient interfaces exist at various transverse locations in the shear flow region.

4) The refractive-index gradient magnitude exhibits variations along the high-gradient interfaces.

Note that these observations refer to the instantaneous spatial structure of the IFT field, and this is practically what is most relevant for aero-optics because it is the instantaneous flow structure that needs to be understood, modeled, and controlled. The ensemble-averaged behavior can be expected of course to be quite different and simpler with smooth ensemble-averaged interfaces.

Observation 1 refers to the finding that the high-gradient regions are spatially relatively isolated, as is evident in Fig. 5a. In other words, large parts of the instantaneous flow region have relatively low refractive-gradient magnitudes. The high-gradient regions appear to occupy only a small fraction of the flow region. This is consistent with computational results at low Reynolds numbers in studies by Samtaney et al.,[24] who found that regions of high-gradient magnitudes in isotropic and homogeneous turbulence occupy a relatively small fraction of the flow.

Observation 2 indicates, furthermore, that the high-gradient regions are not only spatially isolated but are sheetlike, that is, these regions are confined to thin layers in the turbulent flow region. These high-gradient regions can be thought of physically, therefore, as locally thin interfaces. Sheetlike structure, in three-dimensional space, is consistent with the stringlike structure evident in the two-dimensional spatial images or slices such as Fig. 5a.

Observation 3 is particularly important because it illustrates a major qualitative difference between high-compressibility shear layers

and low-compressibility shear layers. The data indicate that the high-gradient interfaces, although spatially isolated and occupying a relatively small fraction of the flow region, are present at several different transverse locations in the instantaneous flow structure, as is evident in the high-compressibility IFT field of Fig. 5a and in direct contrast to the low-compressibility IFT field of Fig. 5b. Whereas at low compressibility the high-gradient interfaces are mostly confined to the instantaneous outer edges of the flow, it is clear that at high compressibility the high-gradient interfaces can be found both in the interior and near the outer boundaries in instantaneous realizations of the flow. This is in sharp contrast with the behavior in low-compressibility turbulent shear layers.[6,7] The comparision of the IFT behavior is evident in Fig. 5b, where isolated high-gradient regions are not found in the interior of the flow, as a result of large-scale organized structures that confine such interfaces mostly to the outer parts of the shear region. At the high-compressibility flow conditions examined presently in Fig. 5a, the high-gradient interfaces are clearly not confined to the outer boundaries of the flow, i.e., they are not excluded from the interior of the flow.

Observation 4 is also important because it indicates that, on the high-gradient interfaces, the refractive-index gradient is not constant, that is, it fluctuates along these interfaces. This must be taken into account if one wishes to model the aero-optical effects of these interfaces, and this will be addressed in the proposed modeling approach in Sec. IV. We note that the variability of the thickness along the high-gradient interfaces is attributable to both intermittency effects associated with the large Reynolds number and the presence of compact shocklets associated with the high compressibility of the flow.

These observations, and the substantial difference between the high-compressibility behavior and the low-compressibility behavior, are shown also in Figs. 6a and 6b. Compare Figs. 6a and 6b with Figs. 5a and 5b, respectively. The observation, at high compressibility, that the high-gradient regions are spatially isolated even though they occupy several transverse locations in the flow, and the interpretation of the optical wavefront phase in terms of the IFT variations indicate that these isolated regions are the dominant elements for the large-scale optical distortions at high compressibility. Whereas the low-gradient regions are of wide transverse extent, and therefore do contribute to the OPL integral, it is the structure of the high-gradient (locally thin) interfaces that can form the basis of a description that captures the large-scale optical distortions, as explained in the modeling approach proposed in the following section.

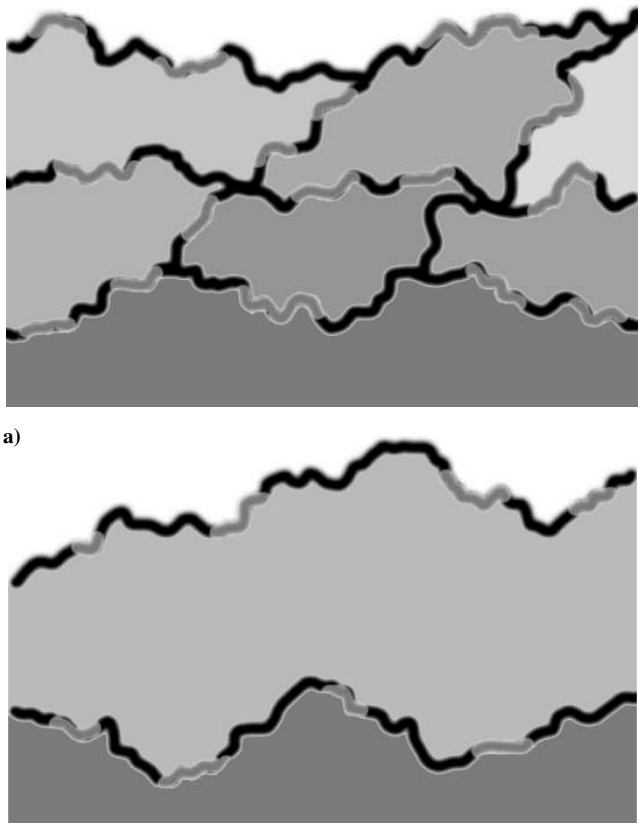

Fig. 6 Schematic of a) network of spatially isolated high-gradient interfaces at high compressibility with variability of IFT along these interfaces indicated and b) high-gradient interfaces at low compressibility.

IV. Proposed Large-Scale Aero-Optics Modeling Approach Based on High-Gradient Interfaces

The observations of the instantaneous structure of the IFT field, in Sec. III, and the interpretation of the OPL in terms of the IFT variations, in Sec. II, can be used to develop a modeling methodology that is useful for capturing the large-scale optical distortions at high compressibility. Before the proposed modeling approach is described, it is helpful to recall the previous work in incompressible and weakly compressible shear layers that has been successful in modeling the large-scale aero-optical distortions. In the case of incompressible shear layers of dissimilar gases, the Brown-Roshko vortical structures[20] generate large-scale regions of nearly uniform refractive index, and this enables the use of the outer interfaces to model the large-scale optical distortions.[6] The outer-interface model of Dimotakis et al.[6] although applicable to low-compressibility mixing cases, does not address the density-field behavior. In the case of weakly compressible shear layers, there are large-scale regions of reduced density and pressure in the flow as shown by Fitzgerald and Jumper.[4] These large-scale reduced density regions can be viewed as weakly compressible analogs of the Brown–Roshko structures. Fitzgerald and Jumper[5] have developed a model based on these large-scale low-density regions, or density wells, and have shown that it is able to reproduce the large-scale optical distortions at low compressibility. The present IFT framework is a general approach and, thus, is not restricted to low compressibilities.

It is known from various investigations of high-compressibility flows that there is a strong qualitative difference between the structure of weakly compressible flows and high-compressibility flows.[9,10,22,23,25,26] For shear layers, in addition to the well-known reduction in the growth rate, there is a substantial difference in the organization of the flow and in particular in the internal structure of the flow as the compressibility level is increased. In particular, accepting the convective Mach number M_c as an adequate measure of compressibility,

$$M_c \equiv (U_1 - U_2)/(a_1 + a_2) \tag{13}$$

where $U_{1,2}$ and $a_{1,2}$ are the freestream speeds and sound speeds, respectively, there is evidence that the flow structure transitions and changes significantly at convective Mach numbers above a certain value.[23] Specifically, in the range

$$M_c \gtrsim 0.6 \tag{14}$$

which corresponds to high compressibility according to most available data, the turbulent flow structure and fluid interfaces appear to be substantially more irregular, and in a qualitatively different way, compared to the behavior at low compressibility.

Comparison of Figs. 5a and 5b, for example, indicates that high-compressibility shear layers exhibit multiple regions spanning different transverse locations where the refractive-index gradients are relatively weak. At the boundaries between these multiple regions, the high-gradient interfaces reside. As discussed in Sec. III, these high-gradient interfaces appear to form a highly irregular network in the flow. Is there a way to model the IFT field at high compressibility to reproduce the aero-optical distortions? In particular, how can the large-scale optical distortions be modeled at high compressibility and which part of the IFT structure is necessary to capture the large-scale optical distortions?

Our proposed modeling approach, at high compressibility, is based on the crucial observation in Sec. III that the high-gradient

interfaces, although located at various transverse locations, are spatially isolated (cf. Figs. 5a and 6a). Because the high-gradient interfaces occupy a relatively small fraction of the total turbulent flow region, we can develop a modeling approach with these interfaces as the dominant elements. A gradient-magnitude threshold is first chosen to identify the high-gradient interfaces. Note that it is crucial to retain the high-gradient interfaces. It may appear, at first sight, that these high-gradient interfaces could be neglected because they only occupy a small fraction of the turbulent flow region. On the contrary, the high-gradient interfaces contribute significantly to the OPL integral because, even though the thickness $h_{n,l}$ is relatively small, the differential $|\mathrm{d}n|$ is relatively large across such interfaces. Thus, the high-gradient interfaces must be included in the modeling approach. Because these interfaces are spatially isolated, it is feasible to approximate the regions in between these interfaces as, for example, zero-gradient regions or uniform-index regions. The next step in the development of this modeling approach is how to propagate the beam through the modeled flow regions. For comparison, in the Ref. 6 modeling approach, the refractive index in the large-scale regions bounded by the outer interfaces is modeled on the basis of the value predicted from the large-scale entrainment. For the present case of high compressibility, however, there are multiple regions through which the beam must be propagated. We propose that the way to do this is to use the gradient information along the high-gradient interfaces to update the refractive index as the OPL integral is computed across these interfaces. The locations of the high-gradient interfaces provide the length scales needed to propagate the beam through the regions in between the interfaces. The proposed modeling approach can be summarized, therefore, in four steps:

1) The high-gradient interfaces are first identified, including their spatial location and gradient values.

2) The optical beam is propagated across the high-gradient interfaces by updating the OPL integral using the gradient values at these interfaces.

3) The regions in between the high-gradient interfaces are modeled as zero-gradient regions.

4) The value of the refractive index in each zero-gradient region, between the high-gradient interfaces, is computed using the gradient value on the interface that the beam propagates across as it enters each zero-gradient region.

A schematic illustrating the basic idea of this model is shown in Fig. 7 for the high-compressibility case. The multiple regions in the interior of the flow are denoted as B–G. We emphasize that it is essential to retain both the location of and gradient values along the high-gradient interfaces in the proposed modeling approach.

The utility of this approach can be demonstrated with the high-compressibility IFT data examined in Sec. III. Figure 8 shows a modeled IFT field, where $\sim$ 50% of the refractive-gradient magnitudes have been set to zero, compared to the original field in Fig. 5a. The OPD integral was computed using this modeled IFT field by following the preceding four steps. The comparison between the full aero-optical wavefront OPD (solid curve) and the modeled OPD (dashed curve) in shown in Fig. 9. Good agreement is evident in terms of the large-scale OPD variations. Different thresholds were examined spanning almost the entire range, that is, from 100 to nearly 0%. As expected, the ability of the thresholded field to capture the large-scale wavefront distortions was found to increase with decreasing threshold. The important finding, however, is that with significant threshold levels one can capture the large-scale wavefront signature. The 50% threshold employed in Fig. 8 is an example illustrating that the high-gradient interfaces contain the essential information to model the large-scale optical distortions. In Fig. 9, the spatial and OPD coordinates are normalized based on large-scale flow extent L_δ. The relatively large OPD rms behavior is due to the use of dissimilar gases with strong differences in the refractive index between the freestreams.

Figure 9 indicates that the proposed modeling approach can be used to reproduce the large-scale optical distortions at high compressibility, in a shear layer, using the high-gradient information. High-gradient interfaces both in the interior and near the outer

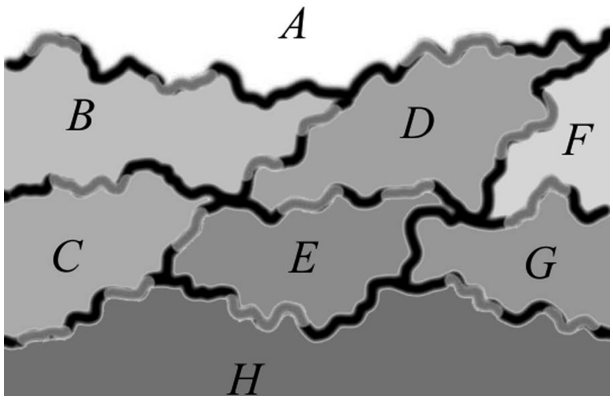

Fig. 7 Interior flow regions B–G that correspond to the low-gradient regions at high compressibility.

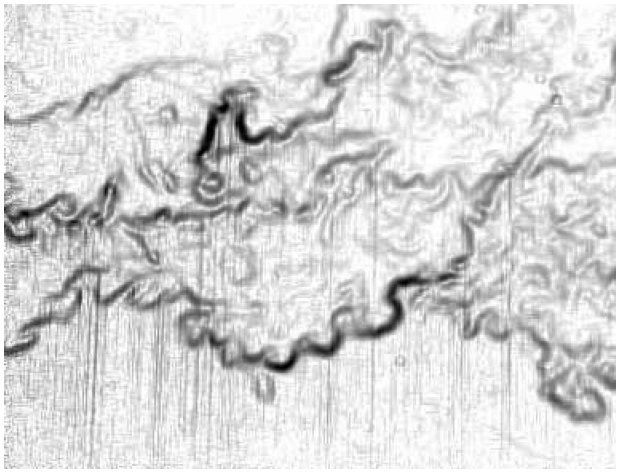

Fig. 8 Modeled IFT field with ∼50% of the gradient magnitudes neglected, at high compressibility.

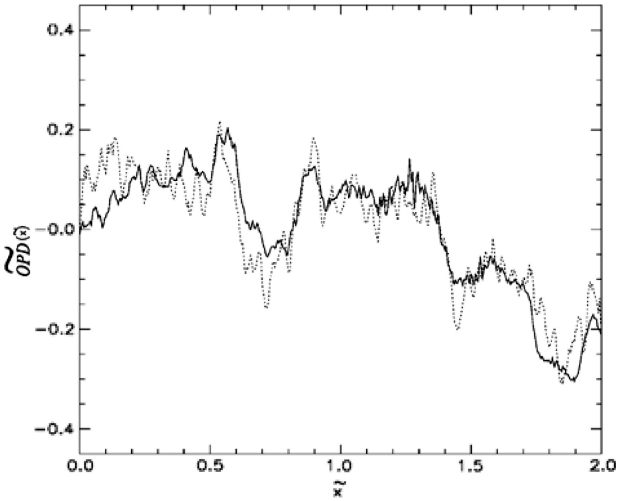

Fig. 9 Comparison of the wavefront OPD, at high compressibility, between ——, full wavefront OPD using the complete IFT field (Fig. 5a), and – – –, modeled OPD using the high-gradient interfaces with ∼50% of the gradient magnitudes neglected (Fig. 8).

boundaries of the flow are essential to capture the large-scale wavefront distortion. However, instead of the full IFT field, information only on the high-gradient interfaces appears to be sufficient to model the large-scale aero-optical distortions. The location of the high-gradient interfaces and the value of the gradient across (or of the thickness of) these interfaces is enough to capture the dominant contributions that generate the large-scale aero-optical distortions. The optical wavefronts are propagated through the high-gradient

(locally thin) interfaces and the gradient value across these interfaces is used to compute the difference in the optical path length, whereas in the low-gradient regions between the high-gradient interfaces the wavefronts are propagated neglecting the presence of the low gradients, that is, as if those regions are zero-gradient regions. The high-gradient interfaces, in this example, are identified in an absolute sense, that is, by thresholding the entire instantaneous gradient field. A further refinement, potentially, could be envisaged by retaining those interfaces that have high gradients relative to their neighboring interfaces. The proposed modeling approach offers a reduction in the amount of flow information needed to capture the large-scale aero-optical distortions at high compressibility. The methodology presented in this work provides a novel point of view with practical benefits in a wide variety of aero-optics applications (e.g., Refs. 27–42).

V. Conclusions

A general IFT approach has been proposed to examine optical-wavefront propagation through turbulent flows in terms of the variability in the physical thickness of the refractive-fluid interfaces. The IFT is given by the inverse of the refractive-index gradient magnitude, and it is highly variable at large Reynolds numbers and high compressibility. The IFT plays a key role in aero-optics because optical wave-fronts physically propagate through variable-thickness refractive interfaces in turbulent flows. The physical role of the IFT is shown by expressing directly the OPL in terms of the IFT variations, in geometrical optics, i.e., ray optics. We have demonstrated the utility of the IFT approach on two-dimensional spatial refractive-field data in shear layers at high compressibility ($M_c \sim 1$) and large Reynolds number ($Re \sim 10^6$). Examination of the in-plane IFT variations revealed that regions of high refractive-gradient magnitudes are located at various transverse locations in the flow, that is, both in the interior and near the outer boundaries, and form highly irregular networks. The high-gradient regions are found to be spatially isolated, that is, occupy a relatively small fraction of the shear layer. This observation, coupled with the interpretation of the OPL in terms of IFT variations, is utilized to propose and demonstrate a new modeling approach, where the high-gradient interfaces are the dominant elements necessary to reproduce the large-scale optical distortions at high compressibility. Both the location of and the gradient values along the high-gradient interfaces are utilized in this modeling approach. As an example, a reduction of $\sim 50\%$ in the amount of interfacial information is able to reproduce well the large-scale optical distortions at high compressibility. The present results suggest applicability of the proposed approach to other high-compressibility flows, by modeling the large-scale optical distortions in terms of the structure of the high-gradient interfaces. The IFT concept proposed and developed in the context of geometrical optics can also be expected to be applicable to Fourier optics or wave optics, for studies of caustics and scattering, as well as for far-field propagation effects. Furthermore, one can anticipate to be able to express the Strehl ratio, which is a related key quantity, in terms of the IFT variations, in a similar manner as was done for the OPL in the present work.

The IFT approach, and its ability to relate the optical behavior to the turbulent IFT variations, can be expected to be helpful in a wide range of studies such as experiments on aero-optical interactions,[27,28] computational modeling and simulations of aero-optics,[29–33] theoretical descriptions and analytical modeling of turbulence effects on beam propagation,[2,34] development of free-space communication systems and optical-imaging techniques,[35–37] two-way coupling of aero-optical interactions, such as in high-energy-laser beam propagation,[38–40] as well as efforts to extend fluid mechanical techniques that suppress or regularize large-scale aero-optical interactions in weakly compressible flows[41,42] to higher flow compressibilities.

Acknowledgments

This work is supported by the Air Force Office of Scientific Research through Grant F49620-02-1-0142 (Thomas Beutner, Program Manager) and is part of a program on aero-optical interactions in turbulent flows. The authors are grateful to Eric Jumper and Demos Kyrazis for their invaluable advice, guidance, and suggestions. The present work is inspired by previous work with Paul Dimotakis and by the early work of Hans Liepmann. Insightful comments by the reviewers are also gratefully acknowledged.

References

[1]Jumper, E. J., and Fitzgerald, E. J., "Recent Advances in Aero-Optics," *Progress in Aerospace Sciences*, Vol. 37, 2001, pp. 299–339.

[2]Kyrazis, D., "Optical Degradation by Turbulent Free Shear Layers," *Optical Diagnostics in Fluid and Thermal Flow*, edited by S. S. Cha and J. D. Trolinger, Society of Photo-Optical Instrumentation Engineers, Bellingham, WA, 1993, pp. 170–181.

[3]Gilbert, K. G., and Otten, L. J., *Aero-Optical Phenomena*, Vol. 80, Progress in Astronautics and Aeronautics, AIAA, New York, 1982.

[4]Fitzgerald, E. J., and Jumper, E. J., "Scaling Aerooptic Aberrations Produced by High-Subsonic-Mach Shear Layers," *AIAA Journal*, Vol. 40, No. 7, 2002, pp. 1373–1381.

[5]Fitzgerald, E. J., and Jumper, E. J., "The Optical Distortion Mechanism in a Nearly Incompressible, Free Shear Layer," *Journal of Fluid Mechanics*, Vol. 512, 2004, pp. 153–189.

[6]Dimotakis, P. E., Catrakis, H. J., and Fourguette, D. C. L., "Flow Structure and Optical Beam Propagation in High-Reynolds-Number Gas-Phase Shear Layers and Jets," *Journal of Fluid Mechanics*, Vol. 433, 2001, pp. 105–134.

[7]Truman, C. R., and Lee, M. J., "Effects of Organized Turbulence Structures on the Phase Distortion in a Coherent Optical Beam Propagating Through a Turbulent Shear Flow," *Physics of Fluids A*, Vol. 2, 1990, pp. 851–857.

[8]Wissler, J. B., and Roshko, A., "Transmission of Thin Light Beams Through Turbulent Mixing Layers," AIAA Paper 92-0658, Jan. 1992.

[9]Papamoschou, D., and Roshko, A., "The Compressible Turbulent Shear Layer: An Experimental Study," *Journal of Fluid Mechanics*, Vol. 197, 1988, pp. 453–477.

[10]Samimy, M., and Elliot, G. S., "Effects of Compressibility on the Characteristics of Free Shear Layers," *AIAA Journal*, Vol. 28, 1990, pp. 439–445.

[11]Smits, A. J., and Dussauge, J.-P., *Turbulent Shear Layers in Supersonic Flow*, AIP Press, Woodbury, NY, 1996.

[12]Aguirre, R. C., and Catrakis, H. J., "Aero-Optical Wavefronts and Scale-Local Characterization in Large-Reynolds-Number Compressible Turbulence," *AIAA Journal*, Vol. 42, No. 10, 2004, pp. 1982–1990.

[13]Liepmann, H. W., "Deflection and Diffusion of a Light Ray Passing Through a Boundary Layer," Douglas Aircraft Co., Rept. SM-14397, Santa Monica, CA, May 1952.

[14]Liepmann, H. W., "Aspects of the Turbulence Problem. Part 1: I. Introduction, II. Stationary Stochastic Processes, III. Turbulence Effects upon Linear Systems." *Zeitschrift für Angewandte Mathematik und Physik*, Vol. 3, 1952, pp. 321–342.

[15]Catrakis, H. J., Aguirre, R. C., Thayne, R. D., McDonald, B. A., and Hearn, J. W., "Are Turbulence-Degraded Optical Wavefronts and Beam Trajectories Fractal?" AIAA Paper 2001-2801, June 2001.

[16]Catrakis, H. J., and Aguirre, R. C., "Inner-Scale Structure of Turbulence-Degraded Optical Wavefronts," AIAA Paper 2002-2269, June 2002.

[17]Aguirre, R. C., Ruiz-Plancarte, J., and Catrakis, H. J., "Physical Thickness of Turbulent Fluid Interfaces: Structure, Variability, and Applications to Aerooptics," AIAA Paper 2003-0642, Jan. 2003.

[18]Sreenivasan, K. R., "Fractals and Multifractals in Fluid Turbulence," *Annual Review Fluid Mechanics*, Vol. 23, 1991, pp. 539–600.

[19]Jumper, E. J., and Hugo, R. J., "Quantification of Aerooptical Phase Distortion Using the Small-Aperture Beam Technique," *AIAA Journal*, Vol. 33, 1995, pp. 2151–2157.

[20]Brown, G. L., and Roshko, A., "On Density Effects and Large Scale Structure in Turbulent Mixing Layers," *Journal of Fluid Mechanics*, Vol. 64, 1974, pp. 775–816.

[21]Chew, L., and Christiansen, W., "Coherent Structure Effects on Optical Performance of Plane Shear Layers," *AIAA Journal*, Vol. 29, 1991, pp. 76–80.

[22]Papamoschou, D., "Structure of the Compressible Turbulent Shear Layer," *AIAA Journal*, Vol. 29, 1991, pp. 680, 681.

[23]Clemens, N. T., and Mungal, M. G., "Large-Scale Structure and Entrainment in the Supersonic Mixing Layer," *Journal of Fluid Mechanics*, Vol. 284, 1995, pp. 171–216.

[24]Samtaney, R., Pullin, D. I., and Kosović, B., "Direct Numerical Simulation of Decaying Compressible Turbulence and Shocklet Statistics," *Physics of Fluids*, Vol. 13, 2001, pp. 1415–1430.

[25]Bogdanoff, D., "Compressibility Effects in Turbulent Shear Layers," *AIAA Journal*, Vol. 21, 1983, pp. 926, 927.

[26]Samimy, M., Reeder, M. F., and Elliot, G. S., "Compressibility Effects on Large Structures in Free Shear Flows," *Physics of Fluids*, Vol. 4, 1992, pp. 1251–1258.

[27]Thurow, B., Samimy, M., Lempert, W., Harris, S. R., Widiker, J., and Duncan, B., "Simultaneous MHz Rate Flow Visualization and Wavefront Sensing for Aerooptics," AIAA Paper 2003-0684, Jan. 2003.

[28]Zaidi, S., Wyckham, C., Miles, R., and Smits, A., "Characterization of Optical Wavefront Distortion due to Boundary Layer at Hypersonic Speeds," AIAA Paper 2003-4308, June 2003.

[29]Elghobashi, S. E., and Wassel, A. T., "The Effect of Turbulent Heat Transfer on the Propagation of an Optical Beam Across Supersonic Boundary/Shear Layers," *International Journal of Heat and Mass Transfer*, Vol. 23, 1980, pp. 1229–1241.

[30]Tsai, Y.-P., and Christiansen, W. H., "Two-Dimensional Numerical Simulation of Shear Layer Optics," *AIAA Journal*, Vol. 28, 1990, p. 2092.

[31]Childs, R. E., "Prediction and Control of Aero-Optical Distortion Using Large-Eddy Simulations," AIAA Paper 1993-2670, June 1993.

[32]Jones, M., and Bender, E. E., "CFD-Based Computer Simulation of Optical Turbulence Through Aircraft Flowfields and Wakes," AIAA Paper 2001-2798, June 2001.

[33]Mani, A., Wang, M., and Moin, P., "Computation of Optical Beam Propagation Through Numerically Simulated Turbulence," *Bulletin of the American Physics Society*, 2003.

[34]Andrews, L. C., and Phillips, R. L., *Laser Beam Propagation Through Random Media*, SPIE Optical Engineering Press, Bellingham, WA, 1998.

[35]Andrews, L. C., Phillips, R. L., and Hopen, C. Y., *Laser Beam Scintillation with Applications*, SPIE Optical Engineering Press, Bellingham, WA, 2001.

[36]Gordeyev, S., Jumper, E. J., Ng, T. T., and Cain, A. B., "Aero-Optical Characteristics of Compressible, Subsonic Turbulent Boundary Layers," AIAA Paper 2003-3606, June 2003.

[37]Kern, B., Dimotakis, P., Lang, D., and Martin, C., "Aberrating Medium Characterization and Image Reconstruction with a Quadrature-Phase Interferometer," AIAA Paper 2003-3610, June 2003.

[38]Fleck, J. A. Jr., Morris, J. R., and Feit, M. D., "Time-Dependent Propagation of High Energy Laser Beams Through the Atmosphere," *Applied Physics*, Vol. 10, 1976, pp. 129–160.

[39]Yahel, R. Z., "Turbulence Effects on High Energy Laser Beam Propagation in the Atmosphere," *Applied Optics*, Vol. 29, 1990, pp. 3088–3095.

[40]Catrakis, H. J., "Turbulence and the Dynamics of Fluid Interfaces with Applications to Mixing and Aero-Optics," *Recent Research Developments in Fluid Dynamics*, edited by N. Ashgriz and R. Anthony, Transworld Research Network, Kerala, India, 2004.

[41]Stanek, M., Sinha, N., Seiner, J., Pearce, B., and Jones, M., "Applying Very High Frequency Excitation to the Problem of Tactical Directed Energy Beam Propagation," AIAA Paper 2002-2272, June 2002.

[42]Siegenthaler, J. P., Jumper, E. J., and Asghar, A., "A Preliminary Study in Regularizing the Coherent Structures in a Planar, Weakly-Compressible, Free Shear Layer," AIAA Paper 2003-0680, Jan. 2003.

H. Atassi
Associate Editor